University of Massachusetts Medical School

eScholarship@UMMS

Rivera Lab Publications

Pediatrics

1997-07-01

Goosecoid and HNF-3beta genetically interact to regulate neural tube patterning during mouse embryogenesis

Stefania Filosa
CNRS/INSERM/Universite Louis Pasteur/College de France

Et al.

Let us know how access to this document benefits you.

Follow this and additional works at: https://escholarship.umassmed.edu/rivera

Part of the Cell Biology Commons

Repository Citation

goosecoid and *HNF-3β* genetically interact to regulate neural tube patterning during mouse embryogenesis

Stefania Filosa[1], Jaime A. Rivera-Pérez[2], Aitana Perea Gómez[1], Anne Gansmuller[1], Hitoshi Sasaki[3], Richard R. Behringer[2] and Siew-Lan Ang[1],*

[1]Institut de Génétique et de Biologie Moléculaire et Cellulaire, CNRS/INSERM/Université Louis Pasteur/Collège de France, BP163, 67404 Illkirch cedex, CU de Strasbourg, France
[2]Department of Molecular Genetics, The University of Texas M. D. Anderson Cancer Center, Houston, Texas 77030, USA
[3]Laboratory of Developmental Biology, Institute for Molecular and Cellular Biology, Osaka University, Osaka 565, Japan

*Author for correspondence (e-mail: siew-lan@igbmc.u-strasbg.fr)

SUMMARY

The homeobox gene *goosecoid* (*gsc*) and the winged-helix gene *Hepatic Nuclear Factor-3β* (*HNF-3β*) are co-expressed in all three germ layers in the anterior primitive streak and at the rostral end of mouse embryos during gastrulation. In this paper, we have tested the possibility of functional synergism or redundancy between these two genes during embryogenesis by generating double-mutant mice for *gsc* and *HNF-3β*. Double-mutant embryos of genotype *gsc*$^{-/-}$;*HNF-3β*$^{+/-}$ show a new phenotype as early as embryonic days 8.75. Loss of *Sonic hedgehog* (*Shh*) and *HNF-3β* expression was observed in the notochord and ventral neural tube of these embryos. These results indicate that *gsc* and *HNF-3β* interact to regulate *Shh* expression and consequently dorsal-ventral patterning in the neural tube. In the forebrain of the mutant embryos, severe growth defects and absence of optic vesicles could involve loss of expression of *fibroblast growth factor-8*, in addition to *Shh*. Our results also suggest that interaction between *gsc* and *HNF-3β* regulates other signalling molecules required for proper development of the foregut, branchial arches and heart.

Key words: *Sonic hedgehog*, *Fgf-8*, neural tube, patterning, forebrain, foregut, *HNF-3β*, *goosecoid*

INTRODUCTION

Early regionalization of the neural tube is characterized by the anterior-posterior (A-P) division of the neural tube into transverse domains, namely forebrain, midbrain, hindbrain and spinal cord and the further subdivision of these regions into dorsal-ventral (D-V) longitudinal domains. Along the A-P axis, this process is revealed in the cephalic neural plate of mouse embryos as early as embryonic day 7.75 (E7.75), by the expression of regulatory genes in distinct domains. For example, the transcription factors Otx2 (Simeone et al., 1993; Ang et al., 1994a), Six3 (Oliver et al., 1995), Fkh2 (Kaestner et al., 1995) and Pax2 (Rowitch et al., 1995) are expressed at the early headfold stage in subdivisions of the presumptive forebrain and midbrain regions. Within the forebrain, further regionalization along the A-P and D-V axes becomes apparent at early somitic stage, with the expression of later markers such as *BF-1* (Tao and Lai., 1992) and *Emx2* (Simeone et al., 1992) which are restricted to the anterior and dorsal part of the forebrain, respectively. Later on, other genes are activated in smaller territories within the telencephalon and diencephalon, further subdividing the forebrain into more transverse and longitudinal domains (reviewed in Rubenstein et al., 1994; Shimamura et al., 1995).

Classical embryological experiments have demonstrated that regionalization of the neural tube along the A-P and D-V axes is regulated by a specialized group of cells called the organizer (reviewed in Kelly and Melton, 1995). Organizer cells have been identified in many vertebrate species, and correspond to the dorsal blastopore lip in *Xenopus*, the Hensen's node in chick, the embryonic shield in zebrafish and the node in mouse. Recent studies have focused on understanding the properties of the organizer at the molecular level. Two classes of genes have been cloned and are implicated in patterning of the A-P axis of the neural tube in *Xenopus* and mouse (reviewed in De Robertis, 1994). One class, encoding nuclear transcription factors, includes the homeobox genes *gsc* and *Otx2*, the winged-helix gene *HNF-3β* and the LIM homeobox gene *Lim1*. The other class encodes signalling molecules such as chordin, follistatin and noggin that can mimic properties of the organizer when administered ectopically to *Xenopus* embryos.

D-V patterning of the neural tube occurs later than A-P patterning and is regulated by axial mesoderm derivatives of the organizer, which form the prechordal mesoderm and notochord. Gene targeting experiments in mice have demonstrated that mutations in *HNF-3β* and the signalling molecule *Sonic hedgehog* (*Shh*), which are both expressed in the prechordal mesoderm and notochord, severely affect D-V patterning of the neural tube (Ang and Rossant, 1994b; Weinstein et al., 1994; Chiang et al., 1996). Moreover, the presence of a single fused optic vesicle in *Shh* mutant mouse embryos (Chiang et al., 1996) and the ectopic expression of *Pax-2* and

suppression of *Pax-6* expression by injections of *Shh* RNA into zebrafish embryos demonstrate an additional role for Shh in eye development (Macdonald et al., 1995). *Shh* has also been shown to induce ventral cell fates of different A-P character in early neural plate or intermediate neural tube explants (reviewed by Placzek, 1995; Tanabe and Jessell, 1996). Transgenic experiments in mice resulting in ectopic expression of *Shh* and *HNF-3β* at the mid-hindbrain junction have shown that *HNF-3β* and *Shh* regulate each other's expression (Echelard et al., 1993; Sasaki and Hogan, 1994; Hynes et al., 1995). Thus, *HNF-3β* and *Shh* represent key components of the ventralising signal emanating from axial mesoderm derivatives.

The in vivo functions of other transcription factors expressed in the organizer have also been investigated in gene targeting experiments. The mutations of *Otx2* and *Lim1* result in a very similar phenotype involving loss of forebrain, midbrain and anterior hindbrain (Shawlot and Behringer, 1995; Acampora et al., 1995; Matsuo et al., 1995; Ang et al., 1996). Although homozygous *HNF-3β* mutants show severe defects in D-V patterning due to the loss of an organised node and of axial mesoderm cells (Ang et al., 1994b; Weinstein et al., 1994), patterning of the neural tube along the A-P axis occurs in mutant embryos from the midbrain to the posterior end of the spinal cord. One possible explanation for this residual A-P patterning activity is that cells with organizer activity remain in the primitive streak of *HNF-3β* mutant embryos. This hypothesis is supported by the observation that *gsc*, which is normally expressed in cells that have the ability to induce an organizer (Blum et al., 1992; Izpisua-Belmonte et al., 1993), is still expressed in *HNF-3β* mutant embryos (Ang et al., 1994b). Null mutations of *gsc* in mice do not affect A-P patterning of the neural tube, but result in craniofacial abnormalities (Rivera-Perez et al., 1995; Yamada et al., 1995), consistent with the later domains of expression of *gsc* (Gaunt et al., 1993). Possible redundant functions of *gsc* and *HNF-3β* have been evoked to explain the lack of phenotype affecting regionalization of the neural tube in *gsc* mutant embryos.

A thorough comparison of the expression patterns of *gsc* and *HNF-3β* has not been reported, although the expression of both *gsc* and *HNF3β* in the anterior primitive streak raised the possibility of genetic interactions between these genes at early stages of gastrulation (Blum et al., 1992; Ang et al., 1993). In this paper, we set out to compare the expression patterns of the two genes to determine the extent of their overlap in E6.5-E9.5 mouse embryos. We found that *gsc* and *HNF3β* are co-expressed not only in cells in the anterior primitive streak of E6.5-E7.5 embryos but also at the anterior end of embryos at E7.75. To determine if the two genes function redundantly or synergistically, we have generated double mutant embryos for *gsc* and *HNF-3β*. Double homozygous mutant embryos are not more severely affected than single *HNF-3β* homozygous mutant embryos in early A-P regionalization of the neural tube, indicating that these genes do not have a redundant function in this process. However, *gsc*$^{-/-}$;*HNF-3β*$^{+/-}$ embryos present a new phenotype as early as E8.75. Analysis of the double-mutant phenotype shows that *gsc* and *HNF-3β* function synergistically in the mouse organizer, forebrain and/or foregut to regulate *Shh* expression and proper development of the neural tube. Our results have thus revealed an earlier role than previously described for *gsc* in growth and patterning of the neural

tube as well as in optic vesicle, foregut, branchial arch, and heart development.

MATERIALS AND METHODS

Generation and genotyping of wild-type and mutant mice

gsc heterozygous mice of 129/Sv × C57BL/6 background (Rivera-Pérez et al., 1995) were crossed with *HNF-3β* heterozygous mice of 129/Sv × CD1 background (Ang and Rossant, 1994b) to generate double heterozygous animals. For genotyping of pups, DNA was extracted from tail tips as described in Laird et al. (1991), and Southern blot analysis was performed as described in Rivera-Pérez et al. (1995) for *gsc* and Ang and Rossant (1994b) for *HNF-3β*. PCR analysis was used to genotype embryos. Yolk sac DNA extraction and PCR for wild-type and mutant *HNF3β* alleles were performed as described in Ang and Rossant (1994b), except that the following primers 5′-GCCCAGAGGACTTGGTGTTG-3′ and 5′-GCAGCG-CATCGCCTTCTATC-3′ were used to detect the mutant allele. The presence of a mutated *gsc* allele was detected using the following primers 5′-AATCCATCTTGTTCAATGGCCGATC-3′, and 5′-TTACAGCTAGCTCCTCGTTGC-3′, to amplify a fragment of 696 bp. For the wild-type *gsc* allele, the following primers were used 5′-GAGCTGCAGCTGCTCAACCAGCTGCACTGT-3′, and 5′-TAG-CATCGACTGTCTGTGCAAGTCC-3′ to amplify a fragment of 743 bp. The DNA was amplified for 35 cycles (94°C/1 minute, 55°C/30 seconds, 72°C/1 minute) in 25 μl volume containing 67 mM Tris HCl, pH 8.8, 6.7 mM MgCl$_2$, 170 μg/ml BSA, 16.6 mM (NH$_4$)$_2$SO$_4$, 1.5 mM dNTPs, 10% DMSO and 0.2 μg of each oligonucleotide.

RNA in situ hybridization, immunohistochemistry and histology

Whole-mount in situ hybridization was performed as described previously (Conlon and Hermann, 1993). For section in situ hybridization, embryos were fixed 1 hour in 4% paraformaldehyde in PBS, equilibrated in 20% sucrose in PBS and embedded in 7.5% gelatin and 14 μm cryosections were cut. In situ hybridization of sections was performed as described in Gradwohl et al. (1996).

The following probes were used: *Pax-2* (Nornes et al., 1990), *Pax-6* (Walter and Gruss, 1991), a 1 kb *gsc* cDNA probe containing the entire coding region, *Shh* (Echelard et al., 1993), *Otx2* (Ang et al., 1994a), *Emx2* (Simeone et al., 1992), *Mox-1* (Candia et al., 1992), *BF-1* (Tao and Lai, 1992), *En-2* (Davis and Joyner, 1988), *Hoxb-1* (Wilkinson et al., 1989), *Fgf-8* (Crossley and Martin, 1995), *Dlx-2* (Price et al., 1991) and *netrin-1* (Serafini et al., 1994).

Whole-mount immunocytochemistry was performed according to published procedures (Davis et al., 1991) using a rabbit polyclonal anti-NKx2.1 (Lazzaro et al., 1991) and anti-HNF-3β antibodies at a dilution of 1:500. After immunocytochemistry or whole-mount in situ hybridization, embryos were postfixed and sectioned in gelatin as described (Gradwohl et al., 1996). Some of the gelatin sections were counterstained for 1 second with hematoxylin.

For histological analysis, embryos at E9.5 were fixed by immersion in 2.5% glutaraldehyde in phosphate-buffered saline (PBS) for 16 hours at 4°C. Embryos were then rinsed in PBS and dehydrated with graded alcohols series and embedded in Epon. 4 μm sections were cut and stained with toluidine blue.

RESULTS

Comparison of *gsc* and HNF-3β expression in mouse embryos from E6.5-E9.5

Earlier studies by different groups have demonstrated that the expression of *gsc* and *HNF-3β* are localised in the anterior

Fig. 1. Comparison of HNF-3β and *gsc* expression in mouse embryos between E6.5 and E8.75. (A) E6.5 embryo stained for *gsc* RNA (purple) and HNF-3β protein (brown). Cells co-expressing HNF-3β and *gsc* (arrow) or uniquely HNF-3β (arrowhead) are found in the anterior part of the primitive streak. (B) A transverse section approximately halfway down the length of the primitive streak of a mid-streak stage embryo shows the presence of cells co-expressing HNF-3β and *gsc* (arrows) and cells expressing only HNF-3β (arrowheads). (C) E8.0 embryo stained for expression of *gsc* and HNF-3β in frontal view. *Mox-1* expression, also analysed in this embryo, is detected in the somites (staining in the lower part of the panel). (D) A transverse section at the level of the forebrain of embryo depicted in C showing co-expression of *gsc* (purple) and HNF-3β (brown) in the ventral forebrain (arrowhead) and foregut (arrow). (E-H) E8.75 embryos. (E) *gsc* is expressed in the ventral diencephalon. (F) HNF-3β is also expressed in the ventral diencephalon and, in addition, in the Rathke's pouch, notochord (arrow) and floor plate. (G) *gsc* is expressed in the oral epithelium (arrow). (H) HNF-3β is also expressed in the oral epithelium (arrow) and in the pharyngeal endoderm, ventral diencephalon and floor plate. Anterior is to the top, except for A where anterior is to the left. Abbreviations: l, left; r, right; di, diencephalon; rp, Rathke's pouch; fp, floor plate and ph, pharynx. Scale bar: 100 μm.
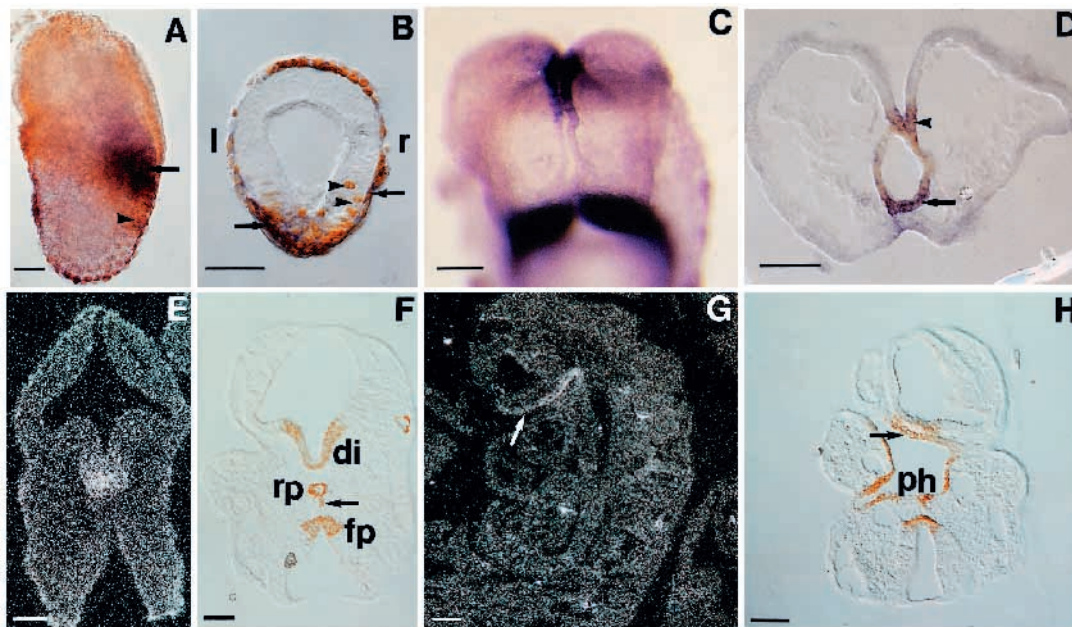
primitive streak during early stages of gastrulation (Blum et al., 1992, Ang et al., 1993; Monaghan et al., 1993). We have compared the expression patterns of the two genes by double-labelling experiments to determine the extent of their overlap. We first analysed expression at E6.0-E6.5, by whole-mount RNA in situ hybridization with a *gsc* cDNA probe followed by whole-mount antibody staining with a HNF-3β specific antiserum. At the early to mid-streak stage, we found co-expression of *gsc* and HNF-3β in many cells in all three germ layers at the anterior end of the primitive streak and in visceral endoderm cells (Fig. 1A,B). Although the domains of expression of the two genes overlap to a large extent, there were also cells expressing uniquely HNF-3β in the ectoderm germ layer, in particular in the distal-most region of the primitive streak (arrowhead in Fig. 1A,B). Thus, *gsc* expression is encompassed within the domain of expression of HNF-3β in the anterior primitive streak.

At headfold (E7.75) and early somite (E8.25) stages, we found a domain of *gsc* expression at the anterior end of the embryo (Fig. 1C,D) that has not been previously reported. As at earlier stages, this domain was contained within the HNF-3β expression domain. Sections through embryos doubly stained for HNF-3β and *gsc* revealed expression of both genes in all three germ layers, i.e in ventral neuroepithelium of the forebrain, prechordal mesoderm and foregut endoderm (Fig. 1D and data not shown). Analysis of *gsc* expression at later stages was performed by radioactive in situ hybridization on tissue sections. In E8.75 embryos, *gsc* expression was observed in the ventral diencephalon (Fig. 1E) and in the oral epithelium (Fig. 1G). Both tissues also expressed HNF-3β (Fig. 1F,H). At

E9.5, the expression of the two genes persisted in the oral epithelium but expression in the diencephalon was no longer detected (data not shown). At E10.5, the patterns of the two genes become distinct, and *gsc* and *HNF-3β* show comple-mentary expression in the mesenchyme and endoderm of the first branchial arch, respectively (Gaunt et al., 1992; Monaghan et al., 1993). We have thus identified domains of *gsc* expression at the rostral end of the embryo from E7.75 to E9.5. In addition, double-labelling studies allow us to conclude that *gsc* and HNF-3β are co-expressed in many cells in the anterior primitive streak and in the forebrain, prechordal mesoderm and foregut endoderm.

Morphological analysis of *gsc* and *HNF-3β* double mutant embryos

The expression of *gsc* and *HNF-3β* in the same cells raised the possibility that these genes interact during early mouse embryonic development. To study genetic interactions between *gsc* and *HNF-3β*, we have generated double heterozygous animals. These animals appeared normal and, when inter-crossed, gave rise to embryos with 9 different genotypes at roughly the expected Mendelian frequencies at E9.5 (Table 1). Embryos with the genotypes *gsc*$^{+/+}$;*HNF-3β*$^{+/-}$, *gsc*$^{+/-}$;*HNF-3β*$^{+/+}$; *gsc*$^{-/-}$;*HNF-3β*$^{+/+}$ and *gsc*$^{+/-}$;*HNF-3β*$^{+/-}$ were mor-phologically normal at this stage. Embryos with four different genotypes were morphologically abnormal and fell into two different classes. One class of embryos, which includes the genotypes *gsc*$^{+/+}$;*HNF-3β*$^{-/-}$, *gsc*$^{+/-}$;*HNF-3β*$^{-/-}$ and *gsc*$^{-/-}$; *HNF-3β*$^{-/-}$, resembled the phenotype of single *HNF-3β* homozygous mutant embryos. These mutant embryos looked

Fig. 2. Mutant phenotypes of embryos generated from a *gsc*^{+/−}*;* *HNF-3β*^{+/−} intercross. (A,B,E-G) E9.5 (C,D) E8.75. (A) *gsc*^{+/+}*;HNF3β*^{−/−} embryo (B) *gsc*^{−/−}*;HNF3β*^{−/−} embryo. Both embryos show development of an A-P axis, with the bulkier end (top) corresponding to the anterior end. (C) Normal E8.75 embryo. (D) *gsc*[/]*;HNF3β*^{+/−} (*gsc/3β*) embryo; defects are apparent in the forebrain, branchial arches and heart. (E) Normal E9.5 embryo. (F) Less severely and (G) more severely affected *gsc/3β* embryos at E9.5. In addition to the defects in the forebrain, branchial arch and heart observed at E8.75, these embryos show posterior defects in the hindbrain, spinal cord and somites (arrowheads). The constriction of the neural tube at the diencephalic-mesencephalic junction (arrowhead in G) is only observed in severely affected embryos. Anterior is to the top. Abbreviations: fb, forebrain; ba, branchial arches; mb, midbrain; hb, hindbrain; ht, heart; ov, optic vesicles; so, somites. Scale bar: 100 μm.
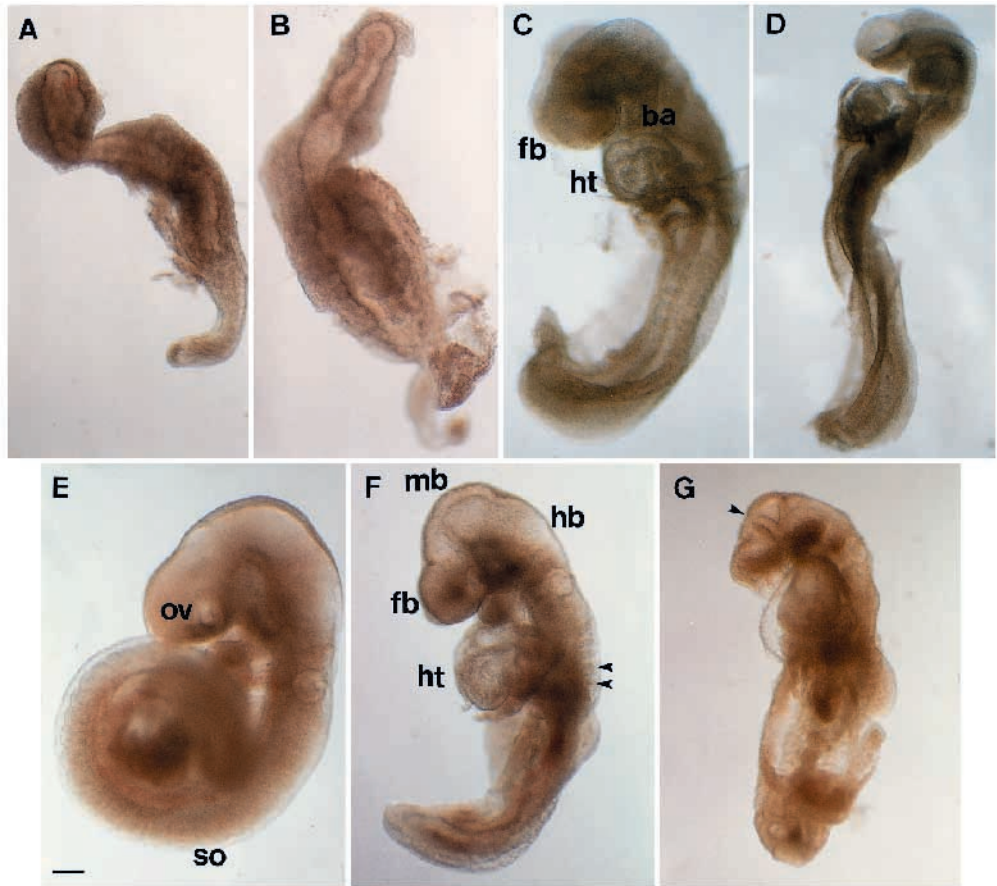
very abnormal, were small and thin with a bulkier end that corresponded to the anterior end of the embryo, as confirmed by the expression of anterior neural markers such as *Emx2* and *Six3* (Fig. 2A,B and data not shown). Importantly, all these embryos, including *gsc*^{−/−}*;HNF-3β*^{−/−} embryos, showed development of an A-P axis and did not appear more severely affected in A-P patterning of the neural tube than single homozygous *HNF-3β* mutant embryos.

The second class of abnormal embryos showed a new phenotype with variable expressivity that has not been previously observed in *HNF-3β* and *gsc* single-mutant studies (Ang et al.; 1994b; Weinstein et al., 1994; Rivera-Pérez et al., 1995; Yamada et al., 1995). All the embryos with this phenotype were genotyped as *gsc*^{−/−}*;HNF-3β*^{+/−} (Fig. 2D,F,G). For simplicity, we will refer to these double-mutant embryos as *gsc/3β* embryos. The *gsc/3β* phenotype was already apparent at E8.75 (14 somites) and was characterised by specific malformations at the anterior end of the embryo, namely a dramatic reduction in forebrain size, abnormal branchial arches and defects in heart looping (Figs 2C,D, 4I,J). No defect was observed further posteriorly and the size of these *gsc/3β* embryos also appeared normal at this stage. At E9.0-9.5, however, *gsc/3β* mutants appeared generally growth-retarded with a reduction in size of the hindbrain, spinal cord and somites (Fig. 2E-G). *gsc/3β* embryos at these stages showed variability in the severity of the mutant phenotype (Fig. 2F,G). The severely affected embryos showed much more dramatic defects in the forebrain, compared to the less severely affected ones. Their forebrain was greatly reduced in size, and the floor and roof of the neural

Table 1. Offspring of *Gsc* and *HNF-3β* mutant mice at E9.5

| Genotype		Frequency	
gsc	*HNF-3β*	Predicted (%)	Observed (%)*·†
+/+	+/+	6.25	8.73
+/+	+/−	12.50	13.49
+/+	−/−	6.25	3.17
+/−	+/+	12.50	12.70
+/−	+/−	25.00	23.81
+/−	−/−	12.50	7.14
−/−	+/+	6.25	7.94
−/−	+/−	12.50	11.90
−/−	−/−	6.25	11.11

*A total of 126 embryos was analyzed.
†The fit to mendelian expectations was tested with a chi-square goodness-of-fit test: χ^2=11.57, df=8, 0.20>*P*>0.10.

tube were in contact with one another at the diencephalic-mesencephalic junction (arrows in Figs 2G, 7K). *gsc/3β* embryos were found in the progeny of double heterozygous intercrosses until E11.5, indicating that these embryos die around this stage. However, they were all developmentally arrested at the 20-25 somite stage. The general growth retardation observed from E9.0 onwards could be a secondary consequence of the heart defects.

Histological analyses of the *gsc/3β* phenotype

To further characterise these mutant defects, semi-thin plastic sections of *gsc/3β* embryos and normal littermates at E9.5 were

Fig. 3. Histological analysis of *gsc/3β* embryos at E9.5. (A,D) Cross-sections of the rostral end of wild-type (A) and *gsc/3β* embryos (D). In a *gsc/3β* embryo, the forebrain and optic vesicles (arrows) are severely reduced in size. Abnormal folds in the walls of the neural tube are occasionally seen in the diencephalon (arrowhead in D). (B,E) Cross-sections at the level of the first and second branchial arches of wild-type (B) and *gsc/3β* embryos (E). Note the presence of pyknotic cells (arrows) in the mesenchyme of the branchial arches, the absence of branchial arch artery and a smaller and abnormally shaped pharynx in the *gsc/3β* embryo. (C,F) Cross-sections at the level of the heart of wild-type (C) and *gsc/3β* embryos (F). The heart is not separated from the gut by the dorsal mesocardium, and the dorsal aorta (arrowheads) appears elongated and disorganized in the *gsc/3β* embryo. The presence of a notochord in *gsc/3β* embryos (D-F) is indicated by open arrowheads. The anterior cardinal veins are also greatly enlarged (arrows). Abbreviations: ov, optic vesicles; no, notochord; ph, pharynx; ba1, branchial arch 1; ba2, branchial arch 2; baa, branchial arch artery; bm, buccopharyngeal membrane; da, dorsal aorta; dm, dorsal mesocardium; en, endocardium; myo, myocardium. Scale bar: 100 μm.
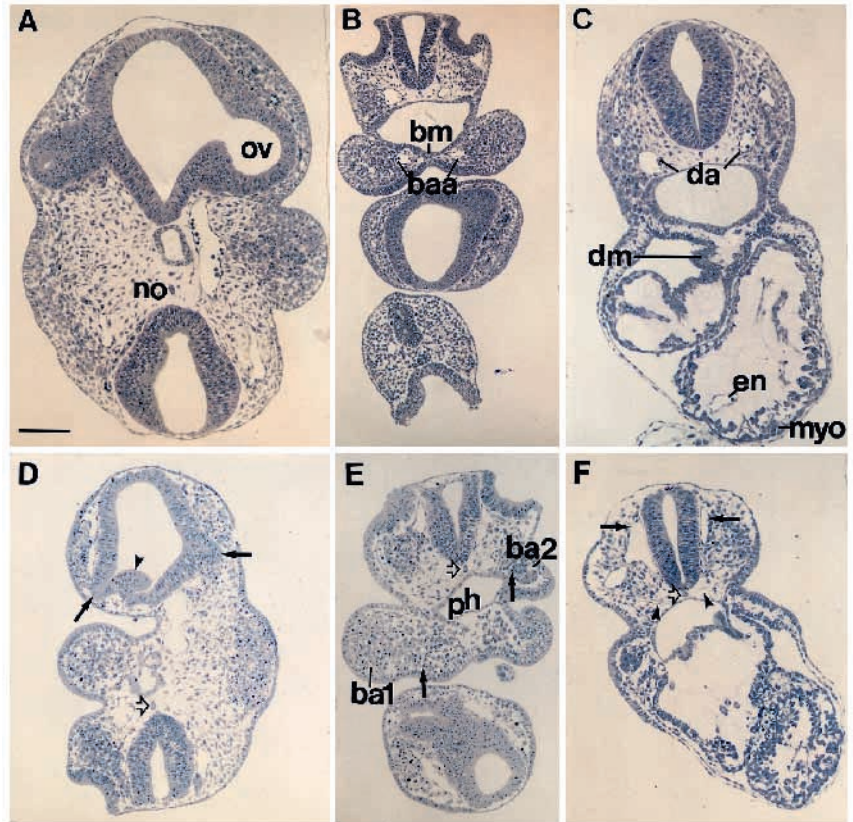
made and processed for histological analysis (Fig. 3). Transverse sections of less severely affected *gsc/3β* mutants at the level of the forebrain clearly showed a thinner neuroepithelium and smaller optic vesicles (Fig. 3A, D). The neuroepithelium of the hindbrain and spinal cord were also thinner compared to normal embryos, but the reduction in size was always more severe and observed earlier in the forebrain region (Fig. 3A-F). In contrast, notochord cells, which fail to develop in single homozygous *HNF-3β* mutant embryos, were clearly observed in transverse sections of *gsc/3β* embryos at different levels along the A-P axis (open arrowheads in Figs. 3D-F). Thus, the neural tube was affected, but axial mesoderm cells were present along the A-P axis in less severely affected *gsc/3β* embryos. In severely affected gsc/3β embryos, however, axial mesoderm cells expressing *HNF-3β* were initially present, but this expression was not maintained and notochord cells subsequently disappeared from the rostral half of these embryos (see below).

Mutant defects were also observed outside of the neural tube. Transverse sections showed the presence of pyknotic cells in the mesenchyme of the first and second branchial arches (Fig. 3B,E). The first branchial arch arteries were either not visible or not well formed and pharyngeal endoderm cells formed a smaller and abnormal pharynx. Furthermore, the epithelium of the first branchial arches did not fuse ventrally with the pharyngeal endoderm to form the buccopharyngeal membrane (Fig. 3B,E). Thus, development of the first and second branchial arches and of the pharynx were severely affected in the *gsc/3β* mutants.

The heart of *gsc/3β* embryos developed as a straight or S-shaped tube in the midline, but failed to loop further (Fig.

2D,F). Transverse sections of *gsc/3β* at the level of the heart showed that the heart was directly connected to the gut, due to the lack of formation of the dorsal mesocardium from splanchnopleuric mesoderm (Fig. 3C,F). The absence of separation between heart and gut could be responsible for the looping defects in the heart. Histological sections also clearly showed an abnormal vasculature. The dorsal aorta was elongated, enlarged or disorganised (Fig. 3C,F and data not shown). These defects could be caused by increased blood pressure resulting from the abnormal heart looping. In contrast, the presence of myogenic and endocardial cells in the heart of *gsc/3β* mutants indicated that development of these two cell types does occur in these embryos (Fig. 3C,F). Thus, the heart problems most likely result secondarily from defects in gut endoderm and dorsal mesocardium development.

Patterning defects in the neural tube

In *Xenopus* and chick embryos, the ability of ectopic *gsc* to induce a secondary neural axis has suggested a role for *gsc* in induction and patterning of the neural tube (Blum et al., 1992; Izpisua-Belmonte et al., 1993). Furthermore, our finding of *gsc* expression in the anterior axial mesendoderm and forebrain of mouse embryos at E7.75 suggested to us that *gsc* may have a role in forebrain development. To determine if A-P patterning of the neural tube was affected in *gsc/3β* embryos, the expression of regional markers specific for distinct domains along the A-P axis was examined. We used the markers *Otx2*, *Emx2* and *BF-1*, for the forebrain region. At E9.5, both *Otx2* and *Emx2* were expressed at the correct A-P level of *gsc/3β* embryos but in a smaller domain, consistent with a reduced size of the forebrain in these embryos (Fig. 4A-D). *BF-1* was
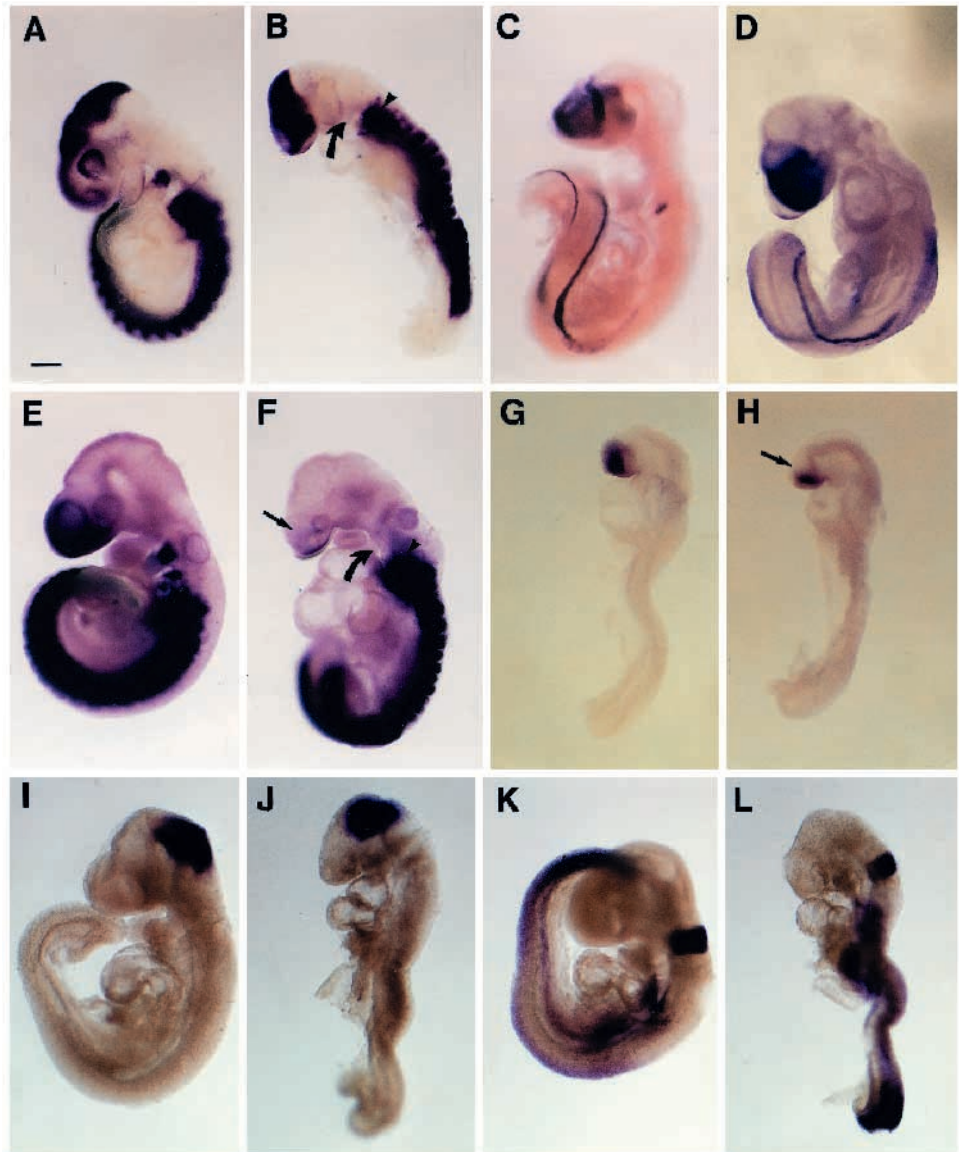
Fig. 4. Whole-mount RNA in situ hybridization of antero-posterior CNS markers. Wild-type (A,C,E,G,I,K) and *gsc/3β* (B,D,F,H,J,L) embryos at E8.75 (G,H) and E9.5 (A-F,I-L). *Otx2* (A,B) and *Emx2* (C,D) are expressed in similar positions along the A-P axis in normal and *gsc/3β* embryos. (E,G) Wild-type *BF-1* expression in the telencephalon. (F,H) *BF-1* expression domain is markedly reduced dorsally in *gsc/3β* mutants (small arrows). (I,J) Similar *En2* expression at the mid-hindbrain junction of wild-type and *gsc/3β* mutants. (K,L) Normal expression of *Hoxb-1* in wild-type and *gsc/3β* mutants. *Mox1* expression was also analysed in some of the embryos (A,B,E,F) to facilitate determination of the number of somites. *Mox1* expression in the second branchial arch is missing in *gsc/3β* embryos (curved arrows in B,F), but its expression in the third and fourth arches appears relatively normal (arrowheads in B,F). Scale bar: 200 μm.

also correctly expressed in the telencephalon of *gsc/3β* embryos at the same stage but its expression domain was markedly reduced dorsally (Fig. 4E,F). This loss of dorsal *BF-1* expression was already detected in E8.75 embryos (Fig. 4G,H). In contrast, expression of *BF-1* in the nasal placode was observed in mutant and normal embryos. To analyse A-P patterning of more posterior regions, *En-2* and *Hoxb1* expression were also examined in *gsc/3β* mutants. Both genes were similarly expressed in *gsc/3β* and wild-type embryos (Fig. 4I-L). Together, these results indicate that A-P patterning of the neural tube occurs normally in *gsc/3β* embryos. In contrast, D-V patterning of the forebrain appears specifically affected.

To further study D-V patterning of the neural tube, we analysed expression of *Pax-6* (Walther and Gruss, 1991) in the alar and basal plates of the neural tube of *gsc/3β* embryos at E9.5. *Pax-6* expression was expanded ventrally in the forebrain, hindbrain and spinal cord in less severely affected *gsc/3β* mutants, when compared to normal littermates (Fig. 5A-D). In the diencephalic region of some severely affected *gsc/3β* embryos, no optic vesicles could be identified morpho-

logically and loss of *Pax-2*, which is expressed in the optic vesicles of normal littermates (Fig. 5E), confirms a loss of these structures (Fig. 5F). Loss of optic vesicles in severely affected *gsc/3β* embryos is not due to a lack of formation but rather to a lack of maintenance of this structure, since optic vesicles are present earlier in these embryos at E8.75 (data not shown). We also studied expression of two homeobox genes that show restricted expression along the D-V ventral axis of the diencephalon, *Dlx-2* (Price et al., 1991) and *Nkx2.1* (Lazzaro et al., 1991). Both genes were expressed in the ventral diencephalon of normal E9.5 littermates but were missing in *gsc/3β* embryos (Fig. 5G,H and I,J respectively). We next examined whether floor plate cells, in the ventral midline of the neural tube, were present in *gsc/3β* mutants, using *netrin-1* (Serafini et al., 1994) as a marker for these cells. *netrin-1* was not expressed in floor plate cells at the anterior end of severely affected *gsc/3β* embryos, whereas expression in the heart and somites was normal (Fig. 5K,L). Thus, analysis of additional D-V molecular markers demonstrated that dorsal cell fates are expanded ventrally, while ventral cell fates, including optic

vesicles in the diencephalon and floor plate cells in the midbrain and hindbrain, are missing in severely affected *gsc/3β* embryos.

Expression of *Shh*, *HNF-3β* and *Fgf-8* are severely affected in *gsc/3β* embryos

One possible explanation for the loss of ventral markers in the neural tube is the absence of a ventralizing signal such as *Shh*, normally provided by the floor plate or the notochord (reviewed in Placzek, 1995; Tanabe and Jessell, 1996). We thus analysed *gsc/3β* mutants at E8.75 for expression of *Shh*, and found it severely reduced or missing at the anterior end, and present to variable levels along the rest of the A-P axis of mutant embryos (Fig. 6C,D and data not shown). Sections through the less severely affected *gsc/3β* embryos at E9.5 showed expression of *Shh* which was weaker than normal in the notochord and barely detectable or absent in the neural tube, except in the diencephalon where *Shh* expression was still present, although at much reduced levels (Fig. 6E-H). *Shh* expression was also missing in the pharyngeal endoderm and in the ventral foregut region (Fig. 6C,D,G,H). Absence or reduction of *Shh* expression was first observed at E8.75 (Fig. 6C,D), whereas its expression was found in the prechordal mesoderm, notochord and foregut at E8.5 (Fig. 6A,B). These results demonstrate that *Shh* expression is initiated in the axial mesoderm and foregut of *gsc/3β* embryos but is not maintained in these tissues anteriorly. *Shh* expression is also severely reduced in the diencephalon and ventral neural tube at E9.5.

Altered expression of *Shh* in *gsc/3β* embryos raised the possibility that *HNF-3β* expression was affected in these embryos, since *HNF-3β* has previously been shown to regulate expression of *Shh* in the neural tube in transgenic mice (Echelard et al., 1993; Hynes et al., 1995). We therefore examined expression of *HNF-3β* in *gsc/3β* embryos between E7.75 and E9.5. *HNF-3β* was normally expressed in the ventral neural tube, prechordal mesoderm, notochord and gut of *gsc/3β* embryos at E7.75-E8.5 (Fig. 7D-F and data not shown), compared to *gsc⁺/⁻;HNF-3β⁺/⁻* littermates (Fig. 7A-C). At E8.75, however, *HNF-3β* expressing cells and a notochord structure were no longer

observed between the neural tube and gut of *gsc/3β* embryos from the heart level to the rostral end (Fig. 7K-M). *HNF-3β* expression was also lost in the ventral neural tube at rostral levels (Fig. 7L,M) and in the oral epithelium (Fig. 7L). In more caudal regions, *HNF-3β* expression was still present in the notochord and floor plate (Fig. 7N). In contrast, *HNF-3β* expression in *gsc⁺/⁻;HNF-3β⁺/⁻* littermates at E8.75 was observed in floor plate, axial mesoderm and gut all along the A-P axis (Fig. 7G-J). *HNF-3β* expression also remained in the gut of gsc/3β embryos at E8.75, although the size, shape and position of the gut were very abnormal (Fig. 7L,M). Thus, expression of *HNF-3β* was initiated normally in the
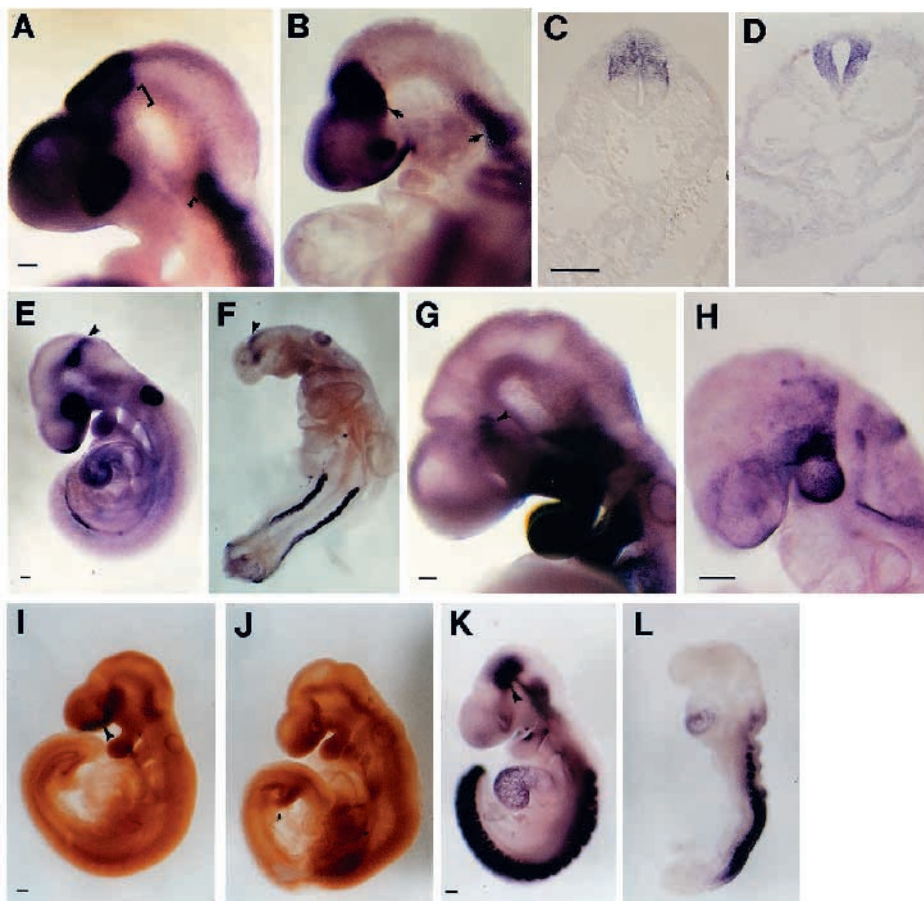

Fig. 5 Whole-mount RNA in situ hybridization and antibody staining of dorso-ventral CNS markers. Wild-type (A,C,E,G,I,K) and *gsc/3β* (B,D,F,H,J,L) embryos at E9.0 to E9.5. (A) Wild-type *Pax-6* expression. (B) *Pax-6* expression domain is expanded ventrally in the forebrain and hindbrain of less severely affected *gsc/3β* mutants (arrows in B). Ventral regions in the neural tube of wild-type embryos that do not express *Pax-6* (A) (demarcated by brackets) are missing in *gsc/3β* embryos (B). (C) Transverse sections showing wild-type *Pax-6* expression in the spinal cord. (D) Expansion of *Pax-6* expression to the ventralmost region of the spinal cord in *gsc/3β* embryos. (E) Wild-type *Pax-2* expression. (F) The expression of *Pax-2* in the optic vesicle is missing in a *gsc/3β* embryo, whereas its expression at the mid-hindbrain junction (arrowhead), otic vesicles and lateral mesoderm is detected. (G) Wild-type *Dlx-2* expression (arrowhead, expression in the ventral diencephalon). (H) In *gsc/3β* embryos, *Dlx-2* expression in the ventral diencephalon is not detected and expression in the branchial arches is severely reduced. In the forebrain region, *Dlx-2* expression was detected in mesenchymal cells. (I) Wild-type *Nkx2.1* expression (arrowhead, expression in the ventral diencephalon). (J) *Nkx2.1* expression in the ventral diencephalon is missing in a *gsc/3β* mutant. (K) Wild-type *netrin-1* expression. (L) In a *gsc/3β* embryo, expression of *netrin-1* is not observed in the anterior neural tube but is present in the somites and heart. Arrowheads in L: normal expression of *netrin-1* in the anterior floorplate. Scale bar: 100 μm.

Fig. 6. Expression of *Shh* in *gsc/3β* embryos. *Shh* expression in E8.5 (A,B), E8.75 (C-D) and (E-H) E9.5 embryos. (A) Wild-type expression of *Shh* in the notochord and foregut at E8.5. (B) At this stage, *Shh* expression in *gsc/3β* mutant embryos is normal. (C) Wild-type expression of *Shh* at E8.75. (D) At this stage, the expression of *Shh* is missing from the notochord and foregut at the anterior end of severely affected *gsc/3β* mutants. (E,G) Wild-type *Shh* expression in transverse sections at brain (E) and spinal cord (G) levels. (F,H) At similar levels in a less severely affected *gsc/3β* embryo, *Shh* expression is reduced in the notochord and diencephalon (open arrow) and very weak or absent in the floor plate (arrowheads) and foregut endoderm (arrow). The distance between notochord and neural tube is increased in some cases in *gsc/3β* embryos (H). Scale bar: 100 μm.
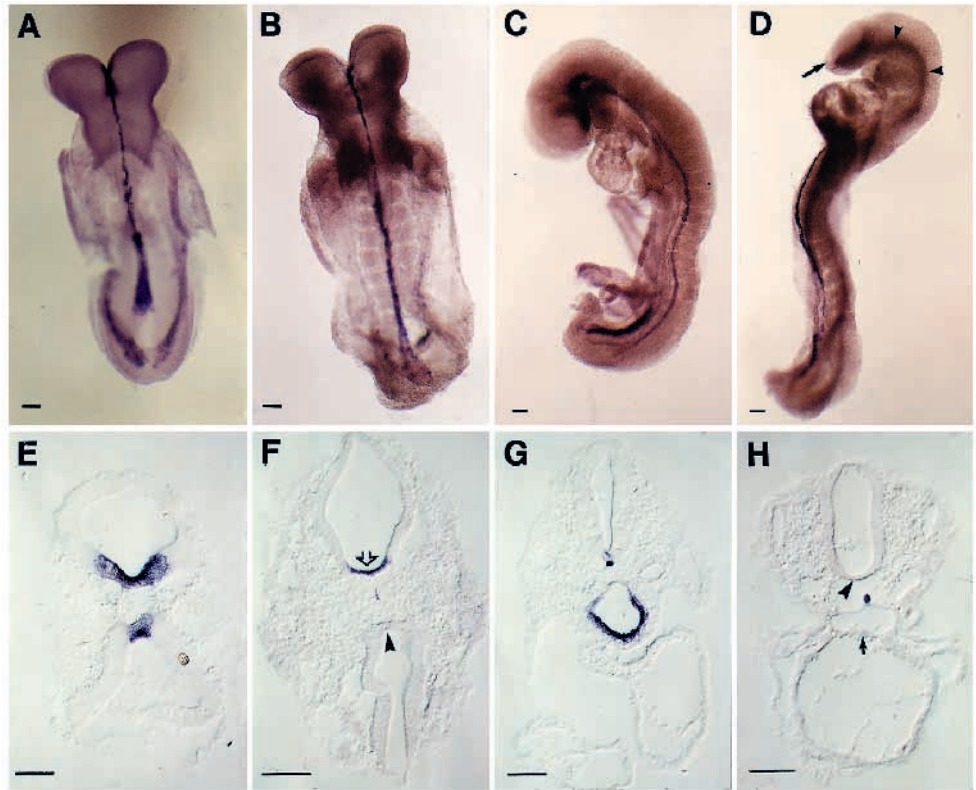
ventral neural tube and axial mesoderm at E8.5, but was not maintained in these tissues subsequently in the rostral half of severely affected *gsc/3β* embryos.

Fibroblast growth factor-8 (FGF-8), another signalling molecule that is expressed in the midbrain and forebrain regions, has been shown to play a key role in regulating growth and polarity in the midbrain (Crossley and Martin, 1995; Crossley et al., 1996; Lee et al., 1997). We have analysed *gsc/3β* mutants for *Fgf-8* expression and found that it was severely affected in the commissural plate of the forebrain. At E8.75, this domain of *Fgf-8* expression appeared reduced in *gsc/3β* mutants compared to wild-type embryos (Fig. 8A,B) and it was no longer detected at E9.5 in severely affected embryos (Fig. 8C,D). In contrast, *Fgf-8* expression in the mid-hindbrain junction, the branchial arches and the tail bud appeared normal. These results demonstrate that, as for *Shh* and HNF-3β, *gsc/3β* embryos initiated but did not maintain *Fgf-8* expression in the forebrain.

Defects in first and second branchial arch development

The first and second branchial arches appeared small and mor-phologically abnormal in the *gsc/3β* mutants at E9.5 (Fig. 2F,G). To determine if mesodermal or neural crest cells were affected in the mutant branchial arches, *Dlx-2* and *Mox-1* were used as markers of these two cell populations, respectively. Expression of *Dlx-2* was severely reduced in the first and second mutant branchial arches (Figs 5G,H). Expression of *Mox1* in the second branchial arch was also severely reduced (arrowheads in Fig. 4B,F), but its expression in the third and fourth branchial arches of mutant embryos appeared relatively normal. Thus, both mesodermal and neural crest cells appear

affected in the first and second branchial arches of *gsc/3β* embryos.

DISCUSSION

Overlapping expression domains of *gsc* and HNF-3β in early mouse embryos

In this paper, we have investigated the possibility of genetic interactions between *gsc* and *HNF-3β* during mouse embryo-genesis by identifying tissues that co-express the two genes and analysing the phenotype of *gsc* and *HNF-3β* double-mutant embryos. Double-labelling studies for *gsc* and HNF-3β expression by whole-mount in situ hybridization and whole-mount antibody staining, indicate that their expression patterns overlap between E6.5 and E8.25. At E6.5, cells in the three germ layers of anterior primitive streak and in the visceral endoderm co-express *gsc* and *HNF-3β*. We also found cells expressing uniquely HNF-3β localized more distally in the embryo. These results demonstrate that cells in the anterior part of the primitive streak are heterogenous in their expression of transcription regulators. It will be important to determine whether this molecular heterogeneity correlates with functional or cell fate differences within the mouse organizer.

We have identified another domain of *gsc* expression at the anterior end of mouse embryos from E7.75 to E8.25, which is very similar to the anterior domain of *gsc* expression in chick and zebrafish embryos (Izpisua-Belmonte et al., 1993; Thisse et al., 1994). In this domain, *gsc* is found in the three germ layers, i.e. in ventral cells of the anterior neural plate, in pre-chordal mesoderm and in foregut, where it is co-expressed with *HNF-3β*. Previous fate-map studies in the chick have demon-

Fig. 7. Expression of HNF-3β in *gsc/3β* embryos. (A) HNF-3β expression in a E8.5 *gsc*⁺/⁻;*HNF-3β*⁺/⁻ control embryo. (B,C) Sections at brain (B) and heart (C) levels of the control embryo shown in A, illustrating expression of HNF-3β in the ventral neural tube (arrowheads), prechordal mesoderm (open arrowhead), notochord (arrow), and gut. (D) HNF-3β expression in a E8.5 *gsc/3β* embryo. (E,F) Sections at brain (E) and heart (F) levels of the *gsc/3β* embryo depicted in D, showing normal HNF-3β expression at this early stage in the ventral neural tube (arrowheads), prechordal plate mesoderm (open arrowhead), notochord (arrow) and gut. (G) HNF-3β expression in a E8.75 *gsc*⁺/⁻;*HNF-3β*⁺/⁻ control embryo. (H-J) Sections at brain (H), heart (I) and spinal cord (J) levels of the control embryo depicted in G, showing expression of HNF-3β in the floor plate (arrowhead), notochord (arrow), foregut and oral epithelium (open arrowhead). (K) HNF-3β expression in a E8.75 *gsc/3β* mutant embryo. The arrow points to a constriction observed in the neural tube around the diencephalic-mesencephalic junction. (L-N) Sections of the *gsc/3β* embryo shown in K. Section at the hindbrain (L) and heart levels (M) showing loss of HNF-3β expression in axial mesoderm, floor plate and oral epithelium (open arrowhead) in the anterior part of the mutant embryo. The first branchial arch of this embryo is fused at the ventral midline (L). (N) A transverse section caudal to the heart, showing that expression of HNF-3β is maintained in the floor plate (arrowhead) and notochord (arrow) in the posterior part of the mutant embryo. Expression of HNF-3β remains in the abnormal gut along the A-P axis (L-N). Abbreviations: hb, hindbrain; nt, neural tube; ba, first branchial arch; g, gut. Scale bar: 100 μm.
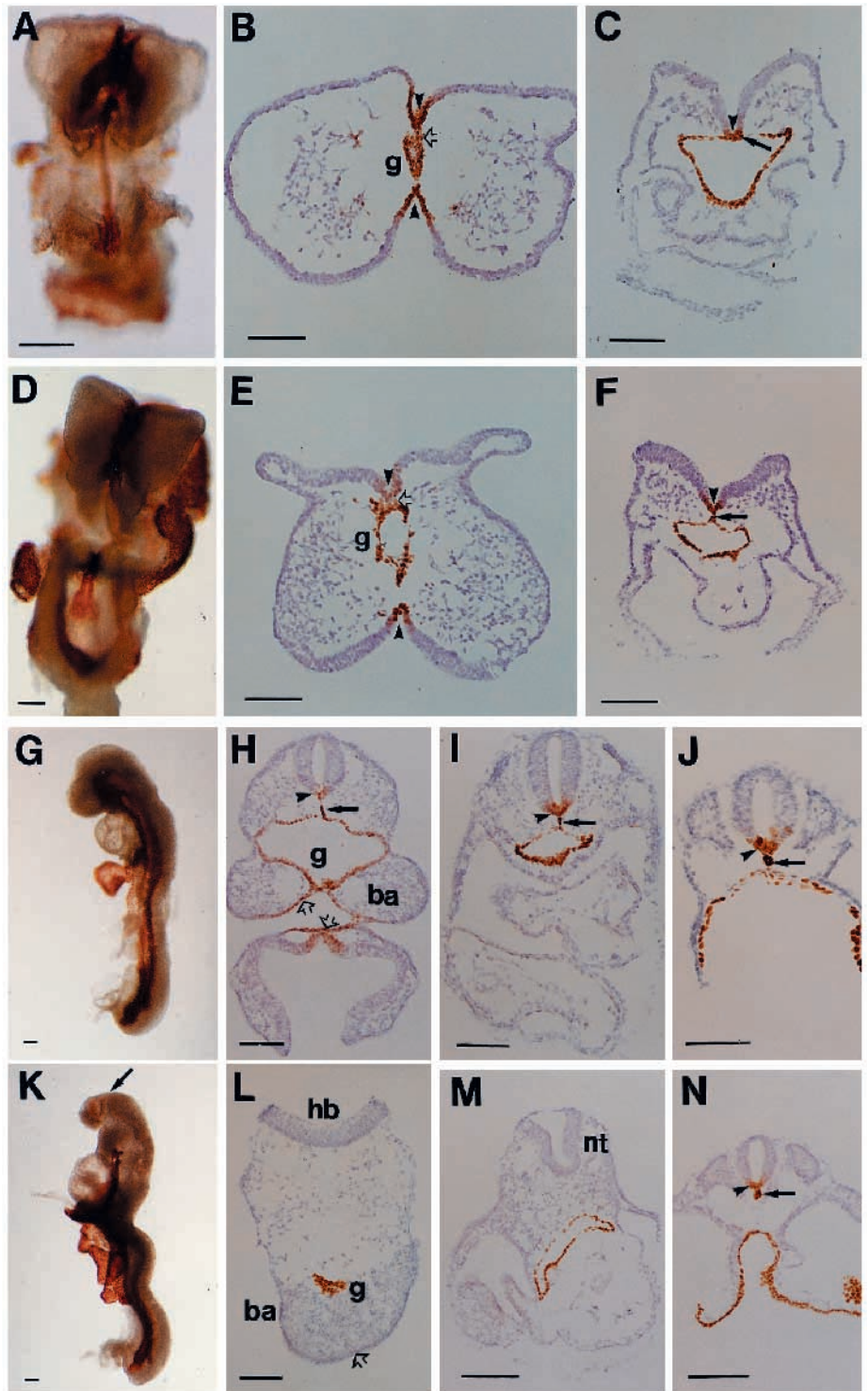
strated that a region similar to the *gsc* domain in the ventral neural plate is fated to form the diencephalon (Couly and le Douarin, 1988). Thus, later *gsc* expression observed in the ventral diencephalon at E8.75 could result from the maintenance of *gsc* expression in the neural plate. *gsc* and *HNF-3β* are also both expressed in the oral epithelium at this stage and at E9.5. In summary, these studies demonstrate that *gsc* and *HNF-3β* are co-expressed in the anterior primitive streak, prechordal mesoderm, forebrain, foregut and oral epithelium from

E6.5 to E9.5, raising the possibility of functional interactions between the two genes in these different tissues.

Dosage-dependent genetic interactions between *gsc* and *HNF-3β* in forebrain and foregut development

Interactions between *gsc* and *HNF-3β* were analysed in *gsc* and *HNF-3β* double-mutant embryos. We did not observe a more severe phenotype in *gsc*⁻/⁻;*HNF3β*⁻/⁻ and *gsc*⁺/⁻;*HNF-3β*⁻/⁻ embryos compared to single homozygous *HNF-3β* mutant

Fig. 8. Expression of *Fgf-8* in *gsc/3β* embryos. (A,C) Wild-type *Fgf-8* expression in the forebrain, mid-hindbrain junction, branchial arches and tailbud of E8.75 (A) and E9.5 (C) embryos. (B,D) In the *gsc/3β* mutant embryos, the expression of *Fgf-8* appears normal in the branchial arches and tailbud but is reduced at E8.75 (B) and undetectable at E9.5 (D) in the forebrain region (arrowhead). Scale bar: 100 µm.

embryos with respect to A-P patterning of the neural tube. Lack of an enhanced phenotype in early A-P axis development indicates that the two genes do not have redundant functions in this process.

Interestingly, however, we observed a new phenotype in embryos with the genotype *gsc⁻/⁻;HNF-3β⁺/⁻*. The earliest morphological defects in these *gsc/3β* embryos were observed at E8.75 in the forebrain, the first branchial arch and the heart. The phenotype in the forebrain of *gsc/3β* embryos is most likely related to the co-expression of *gsc* and *HNF-3β* in this tissue. In the first branchial arches, only the pharyngeal endoderm and the oral epithelium co-express these genes. We thus hypothesize that the branchial arch defects could arise from a primary problem in these two tissues. A foregut defect could also lead to the lack of formation of dorsal mesocardium, and thus secondarily result in heart looping and vasculature defects. *gsc/3β* embryos are growth arrested at 20- to 25-somite stage and die around E11.5. The reasons for the growth retardation and death in the double mutants have not been investigated but could be related to the incomplete heart looping and the vasculature defects.

The new mutant phenotype was only observed in *gsc⁻/⁻;HNF-3β⁺/⁻* embryos, and not in *gsc⁻/⁻* or *HNF-3β⁺/⁻* single mutant embryos. This result and the co-expression of the two genes in the forebrain, foregut and oral epithelium favor the hypothesis of synergistic interactions of *gsc* and *HNF-3β* within the same cells. A normal level of HNF-3β, in the absence of gsc, is sufficient for proper development. However, if only half the normal amount of HNF-3β is present, gsc becomes essential for proper growth and development of these tissues. Haploinsufficiency of *HNF-3β* has previously been demonstrated in *HNF-3β⁺/⁻* animals. In our previous single-mutant study, 20% of *HNF-3β* heterozygous adults had a runted appearance and died within two months of age (Ang et al., 1994b). Furthermore, loss of one dose of HNF-3β leads to changes in the expression of *nodal,* a member of the transforming growth factor-β superfamily of secreted growth factors, and affects the left-right asymmetry of heart looping (Collignon et al., 1996).

Surprisingly, loss of *HNF-3β* expression was observed in the notochord and floor plate of severely affected *gsc/3β* embryos. Thus, a *gsc* null background can lead to loss of *HNF-3β*

expression in the presence of a single copy of the *HNF-3β* gene. No qualitative change in *HNF-3β* expression levels was observed by whole-mount RNA in situ hybridization and whole-mount antibody staining in *gsc⁻/⁻* embryos when two copies of *HNF-3β* were present (data not shown). However, more sensitive methods, such as RNAse protection studies will be necessary to determine whether there are quantitative changes in *HNF-3β* expression in these embryos. Nevertheless, the fact that HNF-3β expression is not maintained in *gsc/3β* embryos demonstrates that *gsc* behaves as a positive regulator of *HNF-3β* expression, when the dosage of *HNF-3β* is lowered. Given that *Shh* and *HNF-3β* expression have been shown to be interdependent (Echelard et al., 1993; Sasaki and Hogan, 1994; Hynes et al., 1995; Chiang et al., 1996), *HNF-3β* expression could be regulated either by direct binding of *gsc* to the *HNF-3β* promoter, or indirectly through regulation of *Shh* by *gsc* (see below).

gsc and *HNF-3β* interact to regulate *Shh* expression in the notochord, forebrain and floor plate of the neural tube

Our phenotypic analyses has revealed that A-P patterning in the neural tube of *gsc/3β* embryos appears normal, whereas D-V patterning present clear defects. In the neural tube, dorsal fates appear to spread ventrally as shown by the expansion of *Pax-6* expression domains. Dorsalization of the forebrain was also confirmed by the loss of expression of the ventral cell fate markers *Dlx-2* and *NKx2.1*. Loss of floor plate development was demonstrated by loss of expression of *HNF-3β*, *netrin-1* and *Shh* in the brain of severely affected *gsc/3β* embryos. Loss of ventral forebrain markers and D-V patterning defects in the neural tube could be due to the loss of or reduction in *Shh* expression observed in *gsc/3β* embryos. This hypothesis is supported by similarities in the forebrain and D-V phenotypes of *gsc/3β* mutants and of the *Shh* homozygous mutants that have been recently been reported (Chiang et al., 1996).

Alterations of *Shh* expression in the foregut and diencephalon of *gsc/3β* embryos strongly suggest that interaction between *gsc* and *HNF-3β* in these tissues is involved in *Shh* regulation. Loss of *Shh* expression is however also observed in the notochord and floor plate, two tissues that express *HNF-3β* but not *gsc*. Lineage studies in mouse have demonstrated that

the precursors of the node and notochord are found exclusively in cells at the anterior primitive streak of E6.5 mouse embryos (Lawson and Pedersen, 1992). This observation indicates that cells in the anterior primitive streak correspond to the early mouse organizer. Thus, one possible explanation for the loss of *Shh* expression in the notochord is that both *gsc* and *HNF-3β* regulate *Shh* in organizer cells at the anterior end of the primitive streak and that loss of *gsc* and of one copy of *HNF-3β* in these organizer cells leads intrinsically to reduced *Shh* expression in their derivatives. Since *Shh* expression in the notochord has been shown to be necessary for induction of floor plate cells in the neural tube (reviewed by Placzek, 1995; Tanabe and Jessell, 1996), loss of *Shh* expression in the notochord is most likely responsible for the loss of *Shh* expression in the neural tube of *gsc/3β* embryos. We have also observed, however, that, in less severely affected *gsc/3β* embryos, *Shh* was expressed in the notochord but not in the neural tube (Fig. 6H). In these cases, loss of *Shh* expression in the neural tube could be explained by reduced *Shh* signalling due to lower levels of *Shh* expression in the notochord and/or to an increased distance between the abnormally positioned notochord and the neural tube (Fig. 6H).

gsc/3β embryos show reduced growth of the telencephalon, diencephalon and optic vesicles. The winged-helix transcription factor *BF-1* has been shown to regulate proliferation of the telencephalic vesicles in mice (Xuan et al., 1994) and loss of its dorsal expression suggest that growth of the dorsal telencephalon may be particularly affected. FGF-8, a molecule with growth-promoting activity in the limb, is also expressed in the forebrain. We have found that the expression of *Fgf-8* in the commissural plate is initiated in *gsc/3β* mutants at E8.75, but is not maintained at E9.5. *Shh* may also have a function in growth of brain tissues since *Shh⁻/⁻* mutant embryos have a reduced brain size (Chiang et al., 1996). Thus, growth defect in the forebrain and lack or abnormal development of the optic vesicles in *gsc/3β* embryos could be caused by the loss of *Fgf-8* and *Shh*. We will test the role of *Shh* and *Fgf-8* in forebrain development by adding recombinant SHH and FGF8 proteins to neural plate explants of *gsc/3β* embryos and assay for the rescue of the forebrain defects.

CONCLUSIONS

gsc and *HNF-3β* genetically interact to regulate development of the neural tube, branchial arches, heart and foregut as early as E8.75, demonstrating an earlier role for *gsc* during embryonic development than determined from single-mutant studies. All *gsc*-expressing cells also express HNF-3β at this early stage, indicating that this interaction results from both genes functioning in the same cells. Furthermore, the loss of *Shh* expression in *gsc/3β* embryos strongly suggests that the activities of both genes in organizer, foregut and forebrain cells converge on the regulation of *Shh* expression. Further studies will be necessary to examine the possibility that the two genes interact directly by binding to the *Shh* promoter. An alternate possibility is that *gsc* regulates *HNF-3β* expression by directly binding to the *HNF-3β* promoter. In this model, we propose that loss of *gsc* expression in *gsc/3β* embryos that contain only one copy of the *HNF-3β* gene, would lead to reduced levels of *HNF-3β* expression beyond a threshold level necessary to

activate an autoregulatory loop. Thus, *HNF-3β* expression is not maintained and consequently leads to a loss of *Shh* expression in these embryos. A third possibility is that *gsc* and *HNF-3β* regulate different target genes in distinct pathways that are both involved in Shh expression.

Our analysis of the *gsc/3β* mutant phenotype also suggests that *Shh* is not the only target gene regulated by *gsc* and *HNF-3β*. For example, severe growth defects in the forebrain and loss of optic vesicles in *gsc/3β* embryos could be caused by loss of expression of both *Fgf-8* and *Shh*, since an abnormal optic vesicle remains in *Shh* mutant embryos (Chiang et al., 1996). In addition, loss of *Shh* expression alone cannot explain the defects seen in the heart and branchial arches, since *Shh* mutant embryos do not show any defects in these tissues at E8.75. It will thus be interesting to investigate in future experiments whether *gsc* and *HNF-3β* interact in the foregut and/or oral epithelium to regulate other signalling molecules that are involved in morphogenesis of the branchial arches and the heart.

REFERENCES

Acampora, D., Mazan, S., Lallemand, Y., Avantaggiato, V., Maury, M., Simeone, A. and Brulet, P. (1995). Forebrain and midbrain regions are deleted in Otx2−/− mutants due to a defective anterior neuroectoderm specification during gastrulation. *Development* **121,** 3279-3290.

Ang, S.-L., Wierda, A., Wong, D., Stevens, K. A., Cascio, S., Rossant, J. and Zaret, K. S. (1993). The formation and maintenance of the definitive endoderm lineage in the mouse: involvement of HNF3/forkhead proteins. *Development* **119,** 1301-1315.

Ang, S.-L., Conlon, R. A., Jin, O. and Rossant, J. (1994a). Positive and negative signals from mesoderm regulates the expression of mouse *Otx2* in ectoderm explants. *Development* **120,** 2979-2989.

Ang, S.-L. and Rossant, J. (1994b). *HNF-3β* is essential for node and notochord formation in mouse development. *Cell* **78,** 561-574.

Ang, S.-L., Jin, O., Rhinn, M,. Daigle, N., Stevenson, L. and Rossant, J. (1996). A targeted mouse *Otx2* mutation leads to severe defects in gastrulation and formation of axial mesoderm and to deletion of rostral brain. *Development* **122,** 243-252.

Blum, M., Gaunt, S. J., Cho, K. W,, Steinbeisser, H., Blumberg, B., Bittner, D. and De Robertis, E. M. (1992). Gastrulation in the mouse: the role of the homeobox gene *goosecoid. Cell* **69,** 1097-2106.

Candia, A. H., Hu, J., Crosby, J., Lalley, P. A., Noden, D., Nadeau, J. H. and Wright, C. V. E. (1992). *Mox-1* and *Mox-2* define a novel homeobox gene subfamily and are differentially expressed during early mesodermal patterning in mouse embryos. *Development* **116,** 1123-1136.

Chiang, C., Litingtung, Y., Lee, K., Young, K. E., Corden, J. L., Westphal, H. and Beach, P. A. (1996). Cyclopia and defective axial patterning in mice lacking Sonic hedgehog gene function. *Nature* **383,** 407-413.

Collignon, J., Varlet, I. and Robertson, E. J. (1996). Relationship between asymmetric nodal expression and the direction of embryonic turning. *Nature* **381,** 155-158.

Conlon, R. A. and Herrmann, B. G. (1993). Detection of messenger RNA by in situ hybridization to postimplantation embryo whole mounts. *Methods Enzymol*. **225,** 373-383.

Crossley, P. H. and Martin, G. R. (1995). The mouse *Fgf-8* gene encodes a family of polypeptides and is expressed in regions that direct outgrowth and patterning in the developing embryo. *Development* **121,** 439-451.

Crossley, P. H., Martinez, S. and Martin, G. R. (1996). Midbrain development induced by FGF8 in the chick embryo. *Nature* **380,** 66-68.

Couly, G. and Le Douarin, N. M. (1988). The fate map of the cephalic neural primordium at the presomitic to the 3-somite stage in the avian embryo. *Development* **103 Supplement**, 101-113.

Davis, C. A. and Joyner, A. L. (1988). Expression patterns of the homeobox-containing genes *En-1* and *En-2* and the proto-oncogene *int-1* diverge during mouse development. *Genes Dev*. **2,** 1736-1744.

Davis, C. A., Holmyard, D. P., Millen, K. J. and Joyner, A. L. (1991). Examining pattern formation in mouse, chicken and frog embryos with an En-specific antiserum. *Development* **111,** 287-298.

De Robertis, E. M. (1994). Dismantling the organizer. *Nature* **374**, 407-408.

Echelard, Y., Epstein, D. J., St-Jacques, B., Shen, L., Mohler, J., McMahon, J. A. and McMahon, A. P. (1993). Sonic Hedgehog, a member of a family of putative signalling molecules, is implicated in the regulation of CNS polarity. *Cell* **75,** 1417-1430.

Gaunt, S. J., Blum, M. and De Robertis, E (1993). Expression of the mouse *goosecoid* gene during mid-embryogenesis may mark mesenchymal cell lineages in the developing head, limbs and body wall. *Development* **117,** 769-778.

Gradwohl, G., Fode, C. and Guillemot, F. (1996). Restricted expression of a novel bHLH atonal-related protein to undifferentiated neural progenitors. *Dev. Biol*. **180,** 227-241.

Hynes, M., Poulsen, K., Tessier-Lavigne, M. and Rosenthal, A. (1995). Control of neuronal diversity by the floor plate: Contact-mediated induction of midbrain dopaminergic neurons. *Cell* **80,** 95-101.

Izpisua-Belmonte, J. C., De Robertis, E. M., Storey, K. G. and Stern, C. D. (1993). The homeobox gene *goosecoid* and the origin of organizer cells in the early chick blastoderm. *Cell* **74,** 645-659.

Kaestner, K. H., Monaghan, A. P., Kern, H., Ang, S.-L., Weitz, S., Lichter, P. and Schutz, G, (1995) The mouse *fkh-2* gene. Implications for notochord, foregut, and midbrain regionalization. *J. Biol. Chem*. **270,** 30029-30035.

Kelly, O. G. and Melton, D. A. (1995). Induction and patterning of the vertebrate nervous system. *Trends Genet*. **11**, 273-278.

Laird, P. W., Zijderveld, A., Linders, K., Rudnicki, M. A., Jaenisch, R. and Berns, A. (1991). Simplified mammalian DNA isolation procedure. *Nucleic Acids Res*. **19**, 4293.

Lawson, K. A. and Pedersen, R. A. (1992). Clonal analysis of epiblast fate during gastrulation and early neurulation in the mouse. In *Postimplantation Development in the Mouse,* Ciba Foundation Symp. **165**, pp 3-26. Chihester:Wiley.

Lazzaro, D., Price, M., de Felice, M. and Di Lauro, R. (1991). The transcription factor TTF-1 is expressed at the onset of thyroid and lung morphogenesis and in restricted regions of the foetal brain. *Development* **113**, 1093-1104.

Lee, S. M. K., Danielian, P. S., Fritzsch, B. and McMahon, A. P. (1997). Evidence that FGF8 signalling from the midbrain-hindbrain junction regulates growth and polarity in the developing midbrain. *Development* **124**, 959-969.

Macdonald, R., Barth B. A., Xu, Q., Mikkola, I. and Wilson, S. W. (1995). Midline signalling is required for Pax gene regulation and patterning of eyes. *Development* **121**, 3267-3278.

Matsuo, I., Kuratani, S., Kimura, C., Takeda, N. and Aizawa, S. (1995). Mouse *Otx2* functions in the formation and patterning of rostral head. *Genes Dev*. **9**, 2646-2658.

Monaghan, A. P., Kaestner, K. H., Grau. E. and Schutz G. (1993). Postimplantation expression patterns indicate a role for the mouse forkhead/HNF-3 alpha, beta and gamma genes in determination of the definitive endoderm, chordamesoderm and neuroectoderm. *Development* **119,** 567-578.

Nornes, H. O., Dressler, G. R., Knapik, E. W., Deutsch, U. and Gruss, P.

(1990) Spatially and temporally restricted expression of Pax2 during murine neurogenesis. *Development* **109**, 797-809.

Oliver, G., Mailhos, A., Wehr, R., Copeland, N. G., Jenkins, N. A. and Gruss, P. (1995). *Six3*, a murine homologue of the *sine oculis* gene, demarcates the most anterior border of the developing neural plate and is expressed during eye development. *Development* **121**, 4045-4055.

Placzek, M. (1995). The role of the notochord and floor plate in inductive interactions. *Curr. Opin. Genet. Dev*. **5**, 499-506.

Price, M., Lemaistre, M., Pischetola, M., Di Lauro, R. and Duboule, D. (1991). A mouse gene related to *Distal-less* shows a restricted expression in the developing forebrain. *Nature* **351**, 748-751.

Rivera-Pérez, J. A., Mallo, M., Gendron-Maguire, M., Gridley, T. and Behringer, R. R. (1995). *Goosecoid* is not an essential component of the mouse gastrula organizer but is required for craniofacial and rib development. *Development* **121**, 3005-3012.

Rowitch, D. H. and McMahon, A. P. (1995). *Pax-2* expression in the murine neural plate precedes and encompasses the expression domains of *Wnt-1* and *En-1*. *Mech.Dev*. **52**, 3-8.

Rubenstein, J. L, Martinez, S., Shimamura, K. and Puelles, L. (1994). The embryonic vertebrate forebrain: the Prosomeric model. *Science* **266**, 578-580.

Sasaki, H. and Hogan, B. L. M. (1994). *HNF-3β* as a regulator of floor plate development. *Cell* **76**, 103-115.

Serafini, T., Kennedy, T., Galko, M., Mirzayan, C., Jessell, T. and Tessier-Lavigne, M. (1994)**.** The netrins define a family of axon-outgrowth-promoting proteins homologous to C. elegans UNC-6. *Cell* **78**, 409-424.

Shawlot, W. and Behringer, R. R. (1995). Requirement for *Lim1* in head-organizer function. *Nature* **374,** 425-430.

Shimamura, K., Hartigan, D. J., Martinez, S., Puelles, L. and Rubenstein, J. L. (1995). Longitudinal organization of the anterior neural plate and neural tube. *Development* **121,** 3923-3933.

Simeone, A., Gulisano, M., Acampora, D., Stornaiuolo, A., Rambaldi, M. and Boncinelli, E. (1992). Two vertebrate homeobox genes related to the Drosophila *empty spiracles* gene are expressed in the embryonic cerebral cortex. *EMBO J*. **11**, 2541-2550.

Simeone, A., Acampora, D., Mallamaci, A., Stornaiuolo. A., D'Apice. M. R., Nigro, V. and Boncinelli, E. (1993). A vertebrate gene related to orthodenticle contains a homeodomain of the bicoid class and demarcates anterior neuroectoderm in the gastrulating mouse embryo. *EMBO J*. **12**, 2735-2747.

Tanabe, Y. and Jessell, T. M. (1996). Diversity and pattern in the developing spinal cord. *Science* **274**, 1115-1123.

Tao, W. and Lai, E. (1992). Telencephalon-restricted expression of *BF-1*, a new member of the HNF-3/fork head gene family, in the developing rat brain. *Neuron* **8,** 957-966.

Thisse, C., Thisse, B., Halpern, M. and Postlethwait, J.H. (1994). *goosecoid* expression in neurectoderm and mesendoderm is disrupted in zebrafish *cyclops* gastrulas. *Dev. Biol*. **164**, 420-429.

Walther, C. and Gruss, P. (1991). *Pax-6*, a murine paired box gene, is expressed in the developing CNS. *Development* **113**, 1435-1449.

Weinstein, D. C., Ruiz i Altaba, A., Chen, W. S., Hoodless, P., Prezioso, V.R., Jessell, T.M. and Darnell, J. E. Jr. (1994). The winged-helix transcription factor *HNF-3β* is required for notochord development in the mouse embryo. *Cell* **78**, 575-588.

Wilkinson, D. G., Bhatt, S., Cook, M., Boncinelli, E. and Krumlauf, R. (1989). Segmental expression of *Hox-2* homeobox genes in the developing mouse hindbrain. *Nature* **341**, 405-409.

Xuan, S., Baptista, C. A., Balas, G., Tao, W., Soares, V. C. and Lai, E. (1994). Winged helix transcription factor BF-1 is essential for the development of the cerebral hemispheres. *Neuron* **14**, 1141-1152.

Yamada, G., Mansouri, A., Torres, M., Stuart, E. T., Blum, M., Schultz, De Robertis, E. M. and Gruss, P. (1995). Targeted mutation of the murine *goosecoid* gene results in craniofacial defects and prenatal death. *Development* **121**, 2917-2922.